



## Experiment Report Form

**The double page inside this form is to be filled in by all users or groups of users who have had access to beam time for measurements at the ESRF.**

Once completed, the report should be submitted electronically to the User Office via the User Portal:

<https://www.esrf.fr/misapps/SMISWebClient/protected/welcome.do>

### ***Reports supporting requests for additional beam time***

Reports can be submitted independently of new proposals – it is necessary simply to indicate the number of the report(s) supporting a new proposal on the proposal form.

The Review Committees reserve the right to reject new proposals from groups who have not reported on the use of beam time allocated previously.

### ***Reports on experiments relating to long term projects***

Proposers awarded beam time for a long term project are required to submit an interim report at the end of each year, irrespective of the number of shifts of beam time they have used.

### ***Published papers***

All users must give proper credit to ESRF staff members and proper mention to ESRF facilities which were essential for the results described in any ensuing publication. Further, they are obliged to send to the Joint ESRF/ ILL library the complete reference and the abstract of all papers appearing in print, and resulting from the use of the ESRF.

Should you wish to make more general comments on the experiment, please note them on the User Evaluation Form, and send both the Report and the Evaluation Form to the User Office.

### **Deadlines for submission of Experimental Reports**

- 1st March for experiments carried out up until June of the previous year;
- 1st September for experiments carried out up until January of the same year.

### **Instructions for preparing your Report**

- fill in a separate form for each project or series of measurements.
- type your report, in English.
- include the reference number of the proposal to which the report refers.
- make sure that the text, tables and figures fit into the space available.
- if your work is published or is in press, you may prefer to paste in the abstract, and add full reference details. If the abstract is in a language other than English, please include an English translation.



	<b>Experiment title:</b> Iron homeostasis in <i>Medicago truncatula</i> nodules	<b>Experiment number:</b> EV246
<b>Beamline:</b> ID21-ID16B	<b>Date of experiment:</b> from: 26/04/2017 to: 05/05/2017	<b>Date of report:</b> 14/09/2017
<b>Shifts:</b> 15(ID21)-3 (ID16B)	<b>Local contact(s):</b> Hiram Castillo (ID21) & Remi Tucoulou (ID16B-NA)	<i>Received at ESRF:</i>
<b>Names and affiliations of applicants (* indicates experimentalists):</b> * Hiram Castillo-Michel, ESRF Manuel Gonzalez-Guerrero, CBGP (UPM-INIA) → <b>Main proposer</b> * Camille Larue * Isidro Abreu Sánchez, CBGP (UPM-INIA) * Patricia Gil Diez, CBGP (UPM-INIA)		

## Report:

**Proposal Summary:** Symbiotic nitrogen fixation (SNF), carried out by the endosymbiotic interaction legumes-rhizobia, is a sustainable source of nitrogen in natural ecosystems and agriculture. For this, transport of iron-species from the host plant to different tissues in the root nodules, where the symbiosis occurs, is fundamental. In this project, we proposed to use  $\mu$ XRF and  $\mu$ XANES to determine Fe distribution and speciation in the context of SNF.

## Results:

**Iron distribution and speciation in *Medicago truncatula*-*Sinorhizobium meliloti* nodule sections:** Previously, we had determined by  $\mu$ XRF that Fe is delivered by the vasculature to a specific zone of model legume *Medicago* nodules. These previous data was obtained from chemically fixed samples (which can suffer artifacts by metal remobilization). Here we used flash-frozen samples, sectioned and analyzed under cryo conditions. Wild type (WT) nodules showed an accumulation of iron in the apical part of the nodule, where the element is present as dots in the apoplast. Then, along the zones of the nodule, we observed an incorporation of iron within the cells, and finally an accumulation of iron in the infected cells, which showed a ring-like distribution typical of symbiosomes (Fig. 1A).

Within nodules, a complex speciation of iron is expected, due to the presence of several iron-chelating molecules (citrate and nicotianamine), and large amounts of ferroproteins, namely cytochromes (containing ionic Fe as cofactor), leghemoglobin (containing heme), and nitrogenase (containing Fe as  $\text{Fe}_4\text{S}_4$  clusters,  $\text{Fe}_8\text{S}_7$  P-clusters and FeMoco cofactor).  $\mu$ XANES data showed that in the vessels, Fe is mainly bound to organic acids as  $\text{Fe}^{3+}$ , or in a form with common aspects with  $\text{Fe}^{2+}$ -S and  $\text{Fe}^{2+}$ -N. In the infection zone (ZII), Fe is mainly associated as  $\text{Fe}^{3+}$  to organic acids (citrate), and a small proportion coordinated as  $\text{Fe}^{2+}$  by sulfur (most likely glutathione). In the interzone and the fixing zone, most of the Fe is present as  $\text{Fe}^{2+}$ , either associated to nitrogen (heme from leghemoglobin or cytochromes), or bound to sulfur (expectedly to Fe-S clusters such as those in nitrogenase) (Fig1D).

**Mutants in iron-chelating molecules alter iron distribution and speciation in nodules:** In *Medicago* there are two main iron chelators: citric acid and nicotianamine. These Fe-binding molecules have an important role in SNF in nodules, since altering their levels in nodules negatively affects symbiosis. However very little information is available of their role and precise. For this we used mutants in a nodule-specific citrate exporter (*mate4-1*) and a nodule-induced NA synthase (*nas1-1*). *mate4-1* showed an altered distribution of iron when compared with WT nodules. Specifically iron is detected in the apoplast, as a dotted pattern similar to that observed in infection zone (ZII) of WT nodules. Furthermore there is a decrease in the incorporation of iron within infected cells (Fig. 1B). In *nas1-1* nodules iron distribution pattern is similar to

WT nodules (Fig. 1C), with three distinguishable zones, but the intensity is half of that observed in WT nodules (data not shown). Interestingly, speciation inferred from  $\mu$ XANES from *mate4-1* and *nas1-1* mutant nodules are similar, and different from that of WT nodules (Fig. 1D). It remains to be determined the reason of this, since citrate and nicotianamine cannot work in the same environment

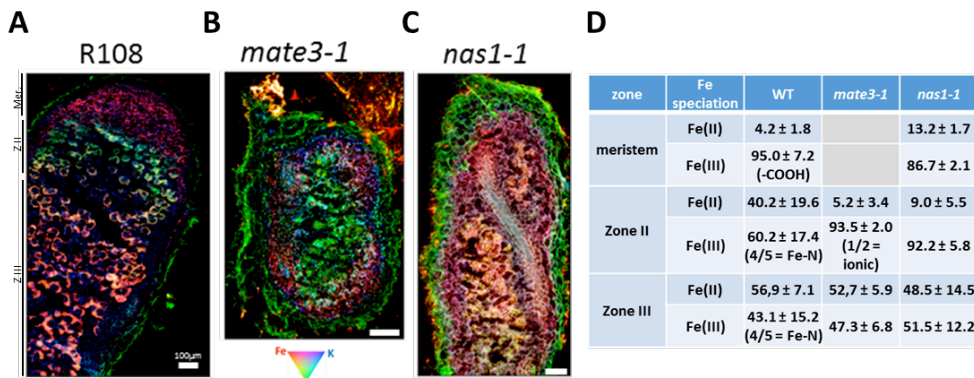


**Figure 1: Iron distribution and speciation in *Medicago* nodules.**

A-C) FeKCa XRF maps of wild type nodules (A), *mate3-1* mutant (B) and *nas1-1* mutant (C). Labels in A indicate different zones in the wild type nodule. Mer, meristem; ZII, zone II or infection/differentiation zone; and ZIII, zone III or fixing zone. Scale bar represent 100 $\mu$ m. D) Summary of Fe species detected by  $\mu$ XANES in samples A to C.

Cryo-setup is required for *in situ* iron speciation analysis: Cryo-techniques are particularly important when analysing metals. Due to their small size and their solubility in water, they are easily mobilized between tissues or subcellular compartments. As a methodology test, we analyzed a same section both in cryohydrated conditions, and after recovery in liquidN<sub>2</sub> followed by liophilization. Iron distribution at tissue level was similar than in fully hydrated samples, even after the distortion in cellular structure observe in freeze-dried samples. In contrast, spectra acquired using pinhole-XANES in both fully-hydrated and liophilized nodule sections, showed that in freeze-dried samples all iron correspond to Fe<sup>3+</sup>.

ID26 Nanobeam allows the detection of metals within bacteroids: As a feasibility test, we used freeze-dried sections at ID16B with the objective of analyze subcellular iron distribution within infected (IC) and non-infected cells (UC). Sections were analyzed with Scanning Electron Microscopy (SEM), showing the existence of some artifacts as the presence of some cavities. However, there is a electrodense network that correspond with symbiosomes (Fig. 2A). XRF maps showed an enrichment of S, Cl, and K in vesicles of UC (Fig. 2B). Metals (Zn, Cu and Fe) were almost absent in UC, but highly accumulated in IC. Specifically, Fe, Cu and Zn are present in the network-like structure corresponding with symbiosomes. Although preliminary, these results suggest an enrichment of metals in symbiosomes, but to advance in that direction we should wait until cryosetup is developed in ID16B line.

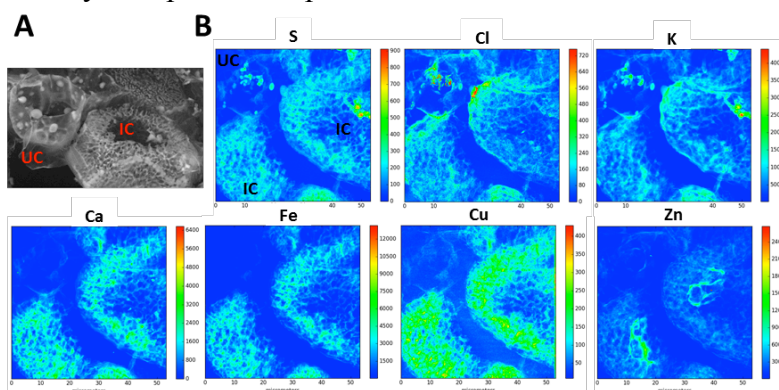


**Figure 2: Iron distribution and speciation in infected and non-infected cells within *Medicago* nodules.**

A) Scanning electron microscopy of freeze-dried nodule sections. B) XRF maps of wild type nodules focused at infected cells (IC) and non-infected cells (UC).

**Conclusions and perspectives:** According to the data obtained in EV-246 experiment, iron shows drastic changes in distribution and oxidation state along the nodule, fitting with the biological processes which are occurring along the nodule. Citrate maintains apoplastic iron in a soluble form because mutants affected in citrate extrusion (*mate4-1*) showed an accumulation of apoplastic iron in a dotted pattern. Surprisingly, mutation of a nicotianamine synthase (*nas1-1*) resulted in a similar localization as in the *mate4-1* plants. However, nicotianamine cannot work in the same environment as citrate. As a tentative model, we propose that nicotianamine is forming a cytosolic iron-pool available for metallation of cytosolic proteins, but this hypothesis would require further experiments. Preliminary data at ID16B showed an enrichment of iron specifically within bacteroids, so our future work will be to identify the plant transporters responsible of metal delivery to symbiosomes and bacteria transporters responsible of uptake from symbiosome space. Overall, these results imply that any biotechnological approach to develop N<sub>2</sub>-fixing plants requires a parallel development of an iron delivery pathway.